

Background field approach to electromagnetic properties of baryons

Tim Ledwig*

Institut für Kernphysik, Universität Mainz, D-55099 Mainz, Germany

(Received 25 November 2011; published 3 May 2012)

We investigate the self-energies of particles in an external magnetic field B . The dependence is generally of the type $\sqrt{P(B)}$ with P a polynomial in B and the participating masses. The nonanalytic point depends on the masses and charges of the involved particles and is unproblematic for stable particles but constrains the linear energy shift approximation for resonances. We recover an earlier reported condition when the self-energy can be expanded in B and derive two more conditions. Furthermore, we obtain the B dependent self-energies of the nucleon and $\Delta(1232)$ -isobar in the $SU(2)$ covariant chiral perturbation theory.

DOI: 10.1103/PhysRevD.85.094002

PACS numbers: 12.39.Fe, 12.40.-y, 13.40.Em, 14.20.Dh

I. INTRODUCTION

Electromagnetic (EM) moments of particles are fundamental observables for their internal structure. Prominent ways to investigate those of baryons are chiral perturbation theories (χ PT) and lattice QCD (IQCD) where two methods are used: the three-point function method, e.g. applied in [1–4], and the background field method, e.g. applied in [5–9]. In this paper we study the self-energies of stable and unstable particles placed in an EM background field from the field theory point of view.

At present, finite volume IQCD results are mainly compared to infinite volume χ PT ones [1–4,10,11] where discrepancies in the small pion mass region can be seen [3,4,11]. Therefore, finite volume corrections on the χ PT side are of interest but reveal certain subtleties. In the case of the three-point function method problems arise for the decomposition of matrix elements in form factors as well as for their Lorentz invariance [12]. A way around this is to obtain these corrections from the self-energy as discussed in [13] for pions. Baryon self-energies in the presence of an external EM field were addressed in [14], however, for the nonrelativistic infinite volume case. A covariant work does not exist, even for the infinite volume, which motivates us to present here the infinite volume nucleon and $\Delta(1232)$ self-energies in the covariant $SU(2)$ χ PT with explicit dependence on a magnetic field.

Another motivation for this work is a deeper study of the nonanalytic EM field dependence of self-energies in field theories [15]. Effects of this nonanalyticity were already encountered for the W boson in the standard model [15–17] and for the $\Delta(1232)$ in χ PT [10,11,18]. Respectively, the quark and pion loop contributions to EM moments diverge for the (albeit unphysical) W -top-bottom and Δ -nucleon-pion mass combinations of $M_W = m_t + m_b$ and $M_\Delta = M_N + m_\pi$. The latter unphysical case is explicitly encountered in the chiral extrapolations of $\Delta(1232)$ EM quantities. Other unstable particles, such as the ρ meson or super symmetric spin 1/2 particles, could exhibit similar

behaviors. Situations would be the EM moments of the ρ with mass $m_\rho = 2m_\pi$ on the lattice, or of the neutralinos (\tilde{N}_i), charginos (\tilde{C}_i) and gluinos whose masses are all unknown [19,20]. For example a \tilde{N} anomalous magnetic moment (AMM) coming from a $W - \tilde{C}$ loop with $M_{\tilde{N}} = M_W + M_{\tilde{C}}$ could be matter of this subject.

For the present analysis we modernize the EM background field technique (BFT) of [21] with which the electron's AMM was correctly obtained for the first time up to the fourth order in 1958. However, it is the three-point function method that afterwards became the preferred method to calculate EM moments. We will use both methods to check our results. It turns out that the self-energies of particles, stable as well as unstable, actually depend non-analytically on the magnetic field B and that conditions for a perturbative treatment exist; one of them studied in [15]. This we also see explicitly for the nucleon and $\Delta(1232)$ -isobar self-energies with $N - \pi$ loops:

$$\Sigma_p(B) = \frac{M_N C_N}{24(1-B)^4} \left[n_1 + n_2 \ln \mu + \frac{n_3}{\sqrt{4\mu^2 - (B + \mu^2)^2}} \arccos \frac{B + \mu^2}{2\mu} \right] + \mathcal{O}(B^2), \quad (1)$$

$$\Sigma_{\Delta^+}(B) = \frac{M_\Delta C_\Delta}{(1-B)^4} \left[d_1 + d_2 \ln \mu + d_3 \ln r + d_4 \ln(1-B) + \frac{(B-1)d_5 \operatorname{arctanh} \omega_1}{\sqrt{\lambda^2 + 4\mu^2 B}} + \frac{(B-1)d_6 \operatorname{arctanh} \omega_2}{\sqrt{\lambda^2 + B(B-2+2r^2+2\mu^2)}} + d_7 \ln(r^2 - B) \right] + \mathcal{O}(B^2), \quad (2)$$

with $\mu = m_\pi/M_N$ and certain polynomials $n_i = n_i(B, \mu)$, $d_i = d_i(B, \mu, r)$, $\lambda^2 = \lambda^2(\mu, r)$ and further nonanalytic functions $\omega_i = \omega_i(B, \mu, r)$ and notations given later. One difference of the self-energies is that the square root in $\Sigma_p(B)$ can be expanded in a weak magnetic field B for all

*ledwig@kph.uni-mainz.de

pion masses $m_\pi > 0$ whereas for the $\Delta(1232)$ -isobar only if the condition

$$\left| \frac{eB}{2M_\Delta} \right| \ll |M_\Delta - (M_N + m_\pi)| \quad (3)$$

between the nucleon, $\Delta(1232)$ and pion masses is met. This is a general situation for unstable particles and was discussed in [15] within a simpler field theory. The work [15] investigates only one Feynman graph whereas we derive here the remaining two conditions coming from the two more Feynman graphs. The mass ratios determine which of the three conditions is the most strict one. Furthermore, we here also study neutral external particles which enables us to estimate when $\mathcal{O}(\mathcal{B}^2)$ terms start to contribute, and derive the above (technically more involved) nucleon and $\Delta(1232)$ self-energies in the covariant $SU(2)$ χ PT.

In the next section necessary notations are given which we use in the third section to study the self-energies of stable and unstable particles. In Secs. IV and V we apply the BFT to the nucleon and $\Delta(1232)$ -isobar.

II. FIELD EQUATIONS IN PRESENCE OF AN EXTERNAL EM FIELD

We consider spin-1/2 and spin-3/2 fields moving in a constant electromagnetic field given by the potential $A_\mu(x) = -\frac{1}{2}F_{\mu\nu}x^\nu$ with $F^{\mu\nu} = \partial^{[\mu}A^{\nu]}$ as the electromagnetic field strength tensor. The Dirac equation for a particle $\Psi(x)$ of mass M with the EM minimal substitution is

$$[\Pi - M]\Psi_A(x) = 0, \quad (4)$$

where we take $e > 0$ and define the momentum $\Pi_\mu = i\partial_\mu - eA_\mu(x)$. This operator is noncommutative with

$$[\Pi_\mu, \Pi_\nu] = \frac{1}{i}F_{\mu\nu}. \quad (5)$$

The spin 3/2 field $\Psi_\mu(x)$ satisfies the equation

$$[\Pi - M]\Psi_A^\mu(x) = 0, \quad (6)$$

with the subsidiary conditions

$$\gamma_\mu \Psi_A^\mu(x) = 0, \quad (7)$$

$$\Pi_\mu \Psi_A^\mu(x) = 0. \quad (8)$$

Because of the noncommutativity of Π we have to symmetrize occurring expressions and use for the propagators:

$$\frac{1}{\Pi - M} = \frac{1}{2} \left[(\Pi + M) \frac{1}{\Pi^2 - M^2 + F} + \frac{1}{\Pi^2 - M^2 + F} (\Pi + M) \right], \quad (9)$$

where we introduce the notation $F = \frac{1}{2i}\gamma^\alpha F_{\alpha\beta}\gamma^\beta$. With this we calculate the particle's self-energy $\Sigma(F)$ and obtain its anomalous magnetic moment (AMM) κ through the linear energy shift [21]:

$$\langle \Psi_A | \Sigma(F) | \Psi_A \rangle = \langle \Sigma(0) \rangle - \langle F \rangle \frac{\kappa}{2M} + \mathcal{O}(F^2). \quad (10)$$

In Fig. 1 we list all Feynman graphs used in this work. The upper row shows all types of graphs that appear to the one-loop level in the BFT, tadpole graphs not considered.

For better reading we use the notation $\vec{B} = M^2 \mathcal{B} \vec{e}_z$, i.e. $\mathcal{B} = |\vec{B}|/M^2$, with which the linear approximation to the self-energy reads:

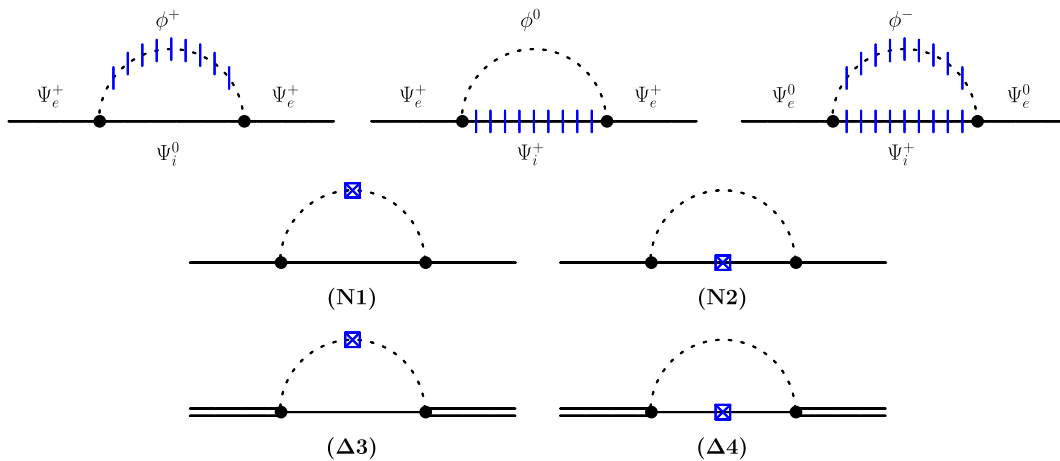


FIG. 1 (color online). Upper row: Feynman graphs contributing to the self-energy in the presence of an external electromagnetic field. The blue lines indicate which loop-internal particle is affected by the field. Middle and lower row: Feynman graphs contributing to the three-point function method to obtain the AMM. Single solid lines correspond to stable particles (e.g. the nucleon), double solid lines to unstable particles (e.g. the $\Delta(1232)$), dashed lines to (pseudo-) scalar particles (e.g. the pion) and the blue cross to the coupling of the photon.

$$\Sigma(B) = \Sigma(0) - M \frac{1}{2} \kappa \mathcal{B} + \mathcal{O}(B^2), \quad (11)$$

$$\Sigma(-B) - \Sigma(B) = M \kappa \mathcal{B} + \mathcal{O}(B^3). \quad (12)$$

The BFT self-energy formulas in this work omit some, but not all, $\mathcal{O}(B^2)$ terms. In particular nonanalytic B structures are preserved in the BFT which are not in the one-photon approximation Eq. (11).

III. SCALAR COUPLINGS AND ESTIMATION OF $\mathcal{O}(B^2)$ EFFECTS

We use the notations of the Appendix and consider two spin 1/2 fields Ψ_1, Ψ_2 interacting with a scalar field ϕ :

$$\begin{aligned} \mathcal{L} = & \sum_{a=1}^2 \bar{\Psi}_a (i \not{D}_a - M_a) \Psi_a + \frac{1}{2} (D_\mu \phi) (D^\mu \phi) \\ & - \frac{1}{2} m^2 \phi^2 + \sum_{a,b=1}^2 g \bar{\Psi}_a \Gamma_{ab} \Psi_b \phi, \end{aligned} \quad (13)$$

with the covariant derivative $D_\mu = \partial_\mu + i q e A_\mu$, q as the charge of the field with $e > 0$ and Γ_{ab} either 1 or γ_5 . In the upper row of Fig. 1 we show the types of self-energy graphs that can occur for a charged or uncharged external particle Ψ_{ex} . The corresponding expressions $\Sigma_i(B)$ with a loop-internal particle Ψ_{in} are

$$\langle \Psi_{\text{ex}} | \Sigma_1(F) | \Psi_{\text{ex}} \rangle = \frac{g^2}{i} \langle \Psi_{\text{ex}} | \int \tilde{d}l \Gamma_1 \frac{1}{[l - M_{\text{in}} + i\varepsilon]} \Gamma_1 \frac{1}{[(\Pi - l)^2 - m^2 + i\varepsilon]} | \Psi_{\text{ex}} \rangle, \quad (14)$$

$$\langle \Psi_{\text{ex}} | \Sigma_2(F) | \Psi_{\text{ex}} \rangle = \frac{g^2}{i} \langle \Psi_{\text{ex}} | \int \tilde{d}l \Gamma_2 \frac{1}{[\Pi - l - M_{\text{in}} + i\varepsilon]} \Gamma_2 \frac{1}{[l^2 - m^2 + i\varepsilon]} | \Psi_{\text{ex}} \rangle, \quad (15)$$

$$\langle \Psi_{\text{ex}} | \Sigma_3(F) | \Psi_{\text{ex}} \rangle = \frac{g^2}{i} \langle \Psi_{\text{ex}} | \int \tilde{d}l \Gamma_3 \frac{1}{[\Pi - l - M_{\text{in}} + i\varepsilon]} \Gamma_3 \frac{1}{[(\Pi_+ + l)^2 - m^2 + i\varepsilon]} | \Psi_{\text{ex}} \rangle, \quad (16)$$

with $\Pi_+^\mu = i\partial^\mu + eA^\mu(x)$. For a third-spin projection of $+1/2$ we can write these expressions in dimensional regularization as

$$\Sigma_i = \frac{-g^2}{(4\pi)^2} M_{\text{ex}} \int_{-\alpha_i}^{1-\alpha_i} dz [s_5(z + \alpha_i) + r] [L + \ln(z^2 - \lambda_i^2 - i\varepsilon) + (\delta_{i1} + \delta_{i2}) \ln(1 - \mathcal{B})] + \mathcal{O}(\mathcal{B}^2), \quad (17)$$

with α_i, λ_i given below and $s_5 = -1$ for $\Gamma_i = \gamma_5$ and $+1$ for $\Gamma_i = 1$. We see that for $\vec{B} = 0$ these expressions are the same and for $\vec{B} \neq 0$ several different logarithms occur. The formula Eq. (17) omits some, but not all, B^2 terms and the integrated solution for the real and imaginary parts are

$$\begin{aligned} \text{Re} \Sigma_i = & \frac{-g^2}{(4\pi)^2} M_{\text{ex}} \left[(s_5 \alpha_i + r) (\beta_i \ln(\beta_i^2 - \lambda_i^2) + \alpha_i \ln(\alpha_i^2 - \lambda_i^2) - 2) + s_5 \frac{1}{2} (\alpha_i^2 - \beta_i^2 + (\beta_i^2 - \lambda_i^2) \ln(\beta_i^2 - \lambda_i^2) \right. \\ & \left. - (\alpha_i^2 - \lambda_i^2) \ln(\alpha_i^2 - \lambda_i^2)) + (\delta_{i1} + \delta_{i2}) \ln(1 - \mathcal{B}) \left(s_5 \alpha_i + r + \frac{s_5}{2} (\beta_i^2 - \alpha_i^2) \right) + (s_5 \alpha_i + r) \Omega_i \right], \end{aligned} \quad (18)$$

$$\text{Im} \Sigma_i = \frac{g^2 \pi}{(4\pi)^2} M_{\text{ex}} (s_5 \alpha_i + r) 2\lambda_i \quad (19)$$

with $\beta_i = 1 - \alpha_i$ and

$$\Omega_i = \begin{cases} 2\sqrt{-\lambda_i^2} \left(\arctan \frac{\beta_i}{\sqrt{-\lambda_i^2}} + \arctan \frac{\alpha_i}{\sqrt{-\lambda_i^2}} \right) & \lambda_i^2 < 0 \\ 2\sqrt{\lambda_i^2} \left(\text{arctanh} \frac{\beta_i}{\sqrt{\lambda_i^2}} + \text{arctanh} \frac{\alpha_i}{\sqrt{\lambda_i^2}} \right) & \lambda_i^2 > 0 \end{cases}, \quad (20)$$

$$\alpha_0 = \frac{1}{2} (1 + r^2 - \mu^2), \quad \lambda_0^2 = \alpha_0^2 - r^2, \quad (21)$$

$$\alpha_1 = \frac{1}{2(1 - \mathcal{B})} (1 + r^2 - \mu^2 - \mathcal{B}), \quad (22)$$

$$\begin{aligned} \lambda_1^2 &= \alpha_1^2 - \frac{r^2}{1 - \mathcal{B}}, \\ \alpha_2 &= \frac{1}{2(1 - \mathcal{B})} (1 + r^2 - \mu^2 - 2\mathcal{B}), \\ \lambda_2^2 &= \alpha_2^2 - \frac{r^2 - \mathcal{B}}{1 - \mathcal{B}}, \end{aligned} \quad (23)$$

$$\alpha_3 = \frac{1}{2} (1 + r^2 - \mu^2 - \mathcal{B}), \quad \lambda_3^2 = \alpha_3^2 - r^2 + \mathcal{B}. \quad (24)$$

The self-energies obtain imaginary parts if λ_i^2 becomes positive together with $-\lambda_i < \beta_i$ and/or $\lambda_i > -\alpha_i$. In addition, the nonanalytic contributions Ω_i give constraints on when the self-energies can be expanded for small \mathcal{B} . These constraints can generically be written as

$$\sqrt{f_i(\mu, r)\mathcal{B} + \lambda_0^2} \rightarrow |\mathcal{B}| < \left| \frac{\lambda_0^2}{f_i(\mu, r)} \right|, \quad (25)$$

for a certain function f_i depending on the type of graph. One of these constraints, coming from the first graph in Fig. 1, was investigated in [15] for the situation of $M_{\text{ex}} > M_{\text{in}}$. A quantitative analysis of the other two graphs, especially the third, was not done. In the following we also study the remaining two graphs as well as further applications of Eq. (17).

A. Nucleon-pion system

The first example is the nucleon-pion (N, π) system with pseudoscalar couplings, $\Gamma_a^{NN\pi} = g_a \gamma_5$. For this we have $s_5 = -1$, $r = 1$, $M_{\text{ex}} = M_N$, $m = m_\pi$ and write for the proton and neutron energies:

$$\Sigma_p(B) = 2\Sigma_1(B) + \Sigma_2(B), \quad (26)$$

$$\Sigma_n(B) = \Sigma_3(0) + 2\Sigma_3(B), \quad (27)$$

with

$$\Sigma_i = \frac{-g^2}{(4\pi)^2} M_N \int_0^1 dz (1-z) \times [L + \ln(z\mu^2 + (1-z)^2 + \mathcal{B}_i - i\varepsilon)], \quad (28)$$

and $\mathcal{B}_1 = z(1-z)\mathcal{B}$, $\mathcal{B}_2 = -(1-z)^2\mathcal{B}$ and $\mathcal{B}_3 = -(1-z)\mathcal{B}$. It is easy to check that we get from this form the same AMM as obtained from the usual three-point function method:

$$\kappa_p = 2\kappa_1 + \kappa_2, \quad \kappa_n = -2\kappa_1 + 2\kappa_2, \quad (29)$$

$$\begin{aligned} \kappa_1 &= \frac{g^2}{(4\pi)^2} \int_0^1 dz \frac{2z(1-z)^2}{z\mu^2 + (1-z)^2}, \\ \kappa_2 &= \frac{g^2}{(4\pi)^2} \int_0^1 dz \frac{-2(1-z)^3}{z\mu^2 + (1-z)^2}. \end{aligned} \quad (30)$$

According to this, we can also write

$$\Sigma_n(B) = 3\Sigma_1(0) - 2\Sigma_1(B) + 2\Sigma_2(B), \quad (31)$$

for the neutron self-energy where the difference of Eq. (31) to Eq. (27) is of order B^2 .

In Fig. 2 we plot the nucleon energy shifts together with the linear approximation with $M_N = 939$ MeV and $m_\pi = 139$ MeV. We see that the signs of the AMM are in agreement with phenomenology, i.e. $\kappa_p > 0$ and $\kappa_n < 0$. To estimate $\mathcal{O}(B^2)$ effects, we use the difference of the red and blue lines in the lower right neutron graph. The com-

bination $\Sigma(-B) - \Sigma(B)$ does not have $\mathcal{O}(B^2)$ contributions whereas the difference of the expressions Eqs. (27) and (31) is of $\mathcal{O}(B^2)$. Plotting the same results for various pion masses shows that the B^2 effects are small for magnetic field strengths of $|B| < \frac{1}{5}M_N^2$ for pion masses larger than $m_\pi = 100$ MeV and for $|B| < \frac{1}{2}M_N^2$ with pion masses around $m_\pi = 600$ MeV. Within these region the Eqs. (11), (27), and (31) give approximately the same results. We estimate therefore that the self-energy formulas are applicable for magnetic field strengths of $|B| < \frac{1}{5}M_N^2$ with pion masses between the physical point $m_\pi = 140$ MeV up to $m_\pi = 600$ MeV. This is the applied pion mass range in lattice QCD calculations.

In addition we also have the nonanalytic \mathcal{B} expressions for the nucleon, Eq. (20), which would constrain a definition of the magnetic moment by the linear energy shift. These constraints read

$$\Sigma_{1,3}: |\mathcal{B}| < |\mu(\mu - 2)|, \quad (32)$$

$$\Sigma_{1,3}: |\mathcal{B}| < |\mu(\mu + 2)|, \quad (33)$$

$$\Sigma_2: |\mathcal{B}| < \left| \frac{1}{4}\mu^2 - 1 \right|, \quad (34)$$

which can always be fulfilled for $0 < \mu < 2$.

Furthermore, we obtain for the nucleon self-energy an imaginary part when a stronger magnetic field is applied. The imaginary parts appear only for $\mathcal{B} \leq -\mu(2 + \mu)$ in Σ_1 and $\mathcal{B} \geq \mu(2 - \mu)$ in Σ_3 .

To see the cause of this we take the present three energy scale problem as a two energy scale problem of some effective values, i.e. modeling the field strength dependence by altering the pion and nucleon masses in a zero magnetic field. This view approximates the real situation of Fig. 2 at small field strengths, e.g. $|\mathcal{B}| < 0.2$, and is meant to give a qualitative insight only. For Σ_1 the magnetic field enters through the pion propagator and we choose to vary the pion mass. Qualitatively, the negative \mathcal{B} side ($-0.3 < \mathcal{B} < 0$) corresponds to a smaller pion mass and the positive \mathcal{B} side ($0 < \mathcal{B}$) to a larger pion mass. An imaginary part is obtained through a complex pion mass which would correspond to a strong negative field ($\mathcal{B} < -0.3$). For the latter pion mass it would be energetically possible for the nucleon and pion inside the loop to go on-shell. However, this would correspond to a pion photoproduction without any excess of energy [22] and is in the present framework unphysical. This situation cannot occur for positive \mathcal{B} since the corresponding effective pion mass gets larger and the $N - \pi$ loop can therefore not open. Furthermore, an imaginary part for Σ_2 is not obtained for the considered field strengths since we would compare it to the large nucleon mass. The Σ_3 is a combination of both so that for Σ_n a similar discussion as for Σ_1 holds. However, the imaginary parts in Fig. 2 appear in a field strength region where unknown higher order \mathcal{B} terms start to

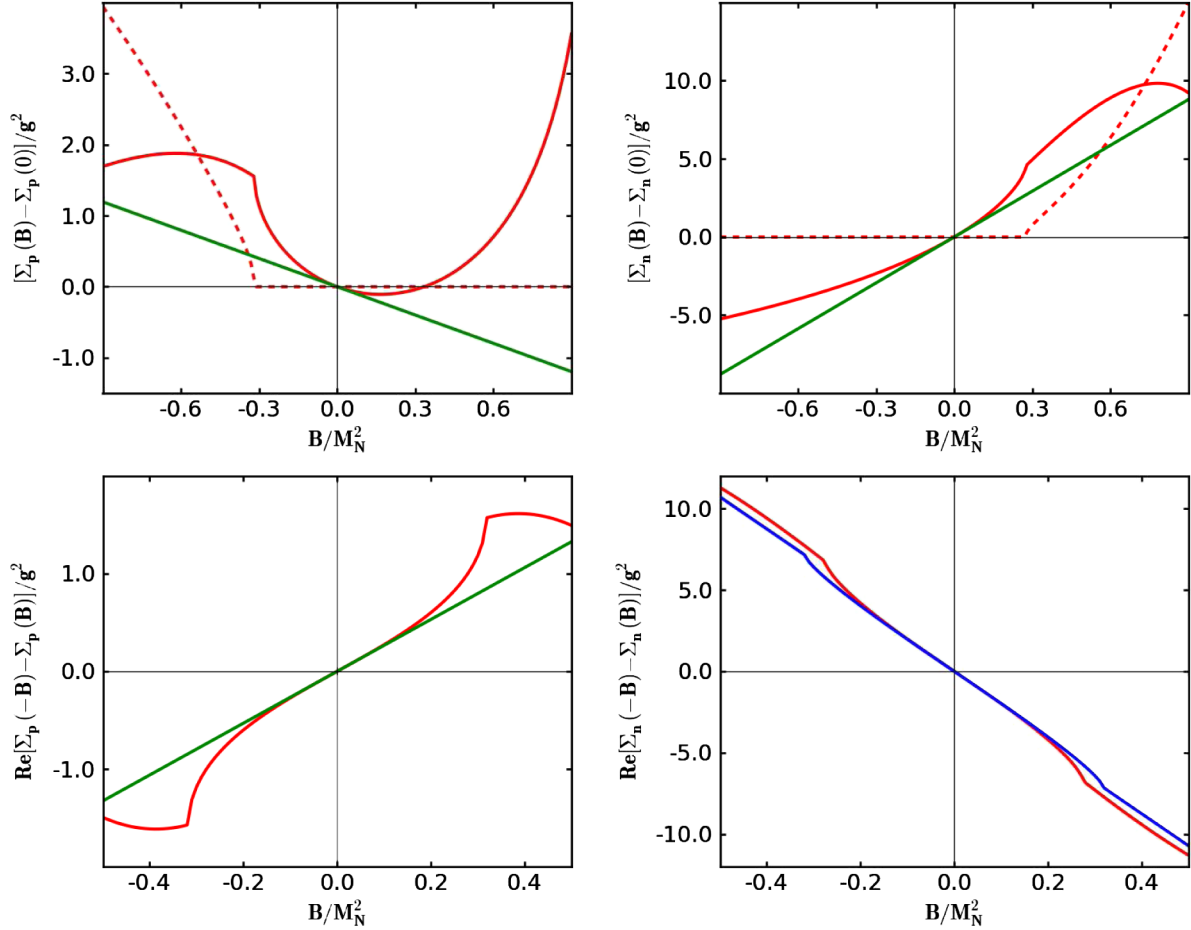


FIG. 2 (color online). Energy shift of the proton (left) and neutron (right) with pseudoscalar coupling for $m_\pi = 139$ MeV. The upper row corresponds to the shift with $\Sigma(B) - \Sigma(0)$ and the lower row to $\Sigma(-B) - \Sigma(B)$. The linear solid green lines correspond to the linear approximation Eq. (11) while the curved solid red lines to Eqs. (26) and (27). The solid blue line shows the result of Eq. (31). The dotted lines correspond to the imaginary parts.

contribute, lower right graph in Fig. 2, and we concentrate on $|\mathcal{B}| < 0.2$.

The nucleon results of this section are obtained from the general expression Eq. (17) for particles with Yukawa couplings as in the Lagrangian Eq. (13) and would be transcriptable for other stable particles in similar field theories.

B. Nucleon-pion-resonance system

For the second example we include a resonance (R) of mass M_R with the coupling $\Gamma_a^{NR\pi} = ig_a$ and get with $s_5 = 1$ and $r = M_N/M_R$ the self-energies:

$$\Sigma_i = \frac{g^2}{(4\pi)^2} M_R \int_0^1 dz (z+r) [L + \ln(z\mu^2 - z(1-z) + (1-z)r^2 + \mathcal{B}_i - i\epsilon)] + \mathcal{O}(B^2). \quad (35)$$

From this, we also recover the results of the three-point method:

$$\begin{aligned} \kappa_1 &= \frac{g^2}{(4\pi)^2} \int_0^1 dz \frac{2z(1-z)(-z-r)}{z\mu^2 - z(1-z) + (1-z)r^2 - i\epsilon}, \\ \kappa_2 &= \frac{g^2}{(4\pi)^2} \int_0^1 dz \frac{2(1-z)^2(z+r)}{z\mu^2 - z(1-z) + (1-z)r^2 - i\epsilon}. \end{aligned} \quad (36)$$

Since the resonance is unstable we have the following imaginary parts for the self-energies:

$$\text{Im } \Sigma_i = -M_R \frac{g^2}{(4\pi)^2} \pi(r + \alpha_i) 2\lambda_i \quad (37)$$

for $\alpha_i > \lambda_i$. Explicitly, these parts are present for magnetic fields of

$$\Sigma_1: \mathcal{B} < -\sqrt{(1-r^2-\mu^2)^2 - 4\lambda_0^2} + 1 - r^2 - \mu^2, \quad (38)$$

$$\Sigma_2: \mathcal{B} > -\frac{\lambda_0^2}{\mu^2}, \quad (39)$$

$$\Sigma_3: \mathcal{B} > +\sqrt{(1-r^2+\mu^2)^2-4\lambda_0^2}-1+r^2+\mu^2. \quad (40)$$

In the case of Σ_2 and Σ_3 with a magnetic field of $\mathcal{B} \geq r^2$ we have $\lambda_i > \alpha_i$, Eq. (37) has to be altered accordingly and an additional cusp is present at $\mathcal{B} = r^2$.

In Fig. 3 we show all three possible self-energies for the parameters $M_N = 939$ MeV, $M_R = 1232$ MeV, and $m_\pi = 139$ MeV together with the linear approximations. For the graph Σ_1 we see the linear behavior near $B = 0$ and a cusp appearing according to Eq. (38). This graph was investigated in [15]. In the case of Σ_2 we see only one cusp at $\mathcal{B} = r^2 \approx 0.6$ since for the present mass combination Eq. (39) is fulfilled for all $|\mathcal{B}| < 1$ and an imaginary part is steadily present. However, choosing m_π closer to the mass-gap $M_R - M_N$ the second cusp appears on the $\mathcal{B} < 0$ side. The occurrence of such two cusps can be seen for Σ_3 . The cusp for $\mathcal{B} < 0$ is due to the imaginary part from Eq. (40) and the one for $\mathcal{B} > 0$ due to $\mathcal{B} \geq r^2$. As we approach with m_π the mass-gap $M_R - M_N$, i.e. $\mu = 1 - r$, all cusps corresponding to Eqs. (38)–(40) converge on $B = 0$ where we have $1 - r - \mu = 0$. For a m_π mass larger than the mass gap the resonance will not be unstable anymore and we get similar results as in the previous example.

To interpret Fig. 3 in physical terms we look once more at the magnetic field as a manipulation of the involved masses. For Σ_1 of Eq. (35) we can again take the quantity $z(1-z)\mathcal{B}$ as a reducing or enhancing term for $z\mu^2$ depending on the sign of \mathcal{B} . On the other hand $z(1-z)$ is also the coefficient in front of the resonance mass term and we could attribute the whole field dependence to a variation of that mass, i.e. $\tilde{M}_R = M_R\sqrt{1-\mathcal{B}}$. This would correspond to an effective heavier resonance for $\mathcal{B} < 0$ and a lighter one for $\mathcal{B} > 0$ whereas the pion and nucleon masses are unaltered. The result is that on the $\mathcal{B} < 0$ side the mass gap is widened and on $\mathcal{B} > 0$ closed. This is exactly the behavior in the left graph of Fig. 3. An imaginary part is usually associated with a decay width and we see that the imaginary part is absent when the mass gap is closed, i.e. no decay is energetically possible, and enhances as the

mass gap enlarges. For Σ_2 the behavior is similar where we absorb the field dependence in an effective resonance mass of $\tilde{M}_R = M_R\sqrt{1-\mathcal{B}}$ together with a nucleon mass of $\tilde{M}_N = M_N\sqrt{r^2-\mathcal{B}}$. For more positive \mathcal{B} the \tilde{M}_N decreases faster than \tilde{M}_R and the decay width enhances as the mass gap grows. At $\mathcal{B} = r^2$ we also see that the effective nucleon mass becomes complex which results in the additional cusp. For Σ_3 the field dependence could be absorbed in $\tilde{M}_N = M_N\sqrt{r^2-\mathcal{B}}$ with the corresponding decay width behavior as in the right graph of Fig. 3.

The above discussion is however meant to be qualitative only. We solely discussed the masses inside the logarithm to grasp the effect induced by the external magnetic field. Qualitatively, the effect is that the involved energy levels are rearranged in a way that either a decay is energetically possible or not depending on the sign of the field strength. The self-energy here depends on the three parameters M_1 , M_2 , m in Eq. (13) and the field strength \mathcal{B} . In contrast to the previous example, even for reasonable mass values can the nonanalytic point be in the $|\mathcal{B}| < 0.2$ region if the mass-gap $M_1 - (M_2 + m)$ is not wide enough.

The explicit conditions to expand the self-energies for small \mathcal{B} due to the nonanalytic contributions Ω_i , Eq. (20), are

$$\Sigma_1: |\mathcal{B}| < 2|1 - r - \mu|, \quad (41)$$

$$\Sigma_2: |\mathcal{B}| < \frac{2r}{1-r}|1 - r - \mu|, \quad (42)$$

$$\Sigma_3: |\mathcal{B}| < 2r|1 - r - \mu|, \quad (43)$$

for the parameters $r < 1$, $\mu > 0$, and $\mu < 1 + r$. The first condition was found in [15]. Which condition is the most strict one depends on the charge of the external particle and the actual values of the masses. For charged external particles with $\mu < r$ and $r > 1/2$ it is the first one and for uncharged the last one.

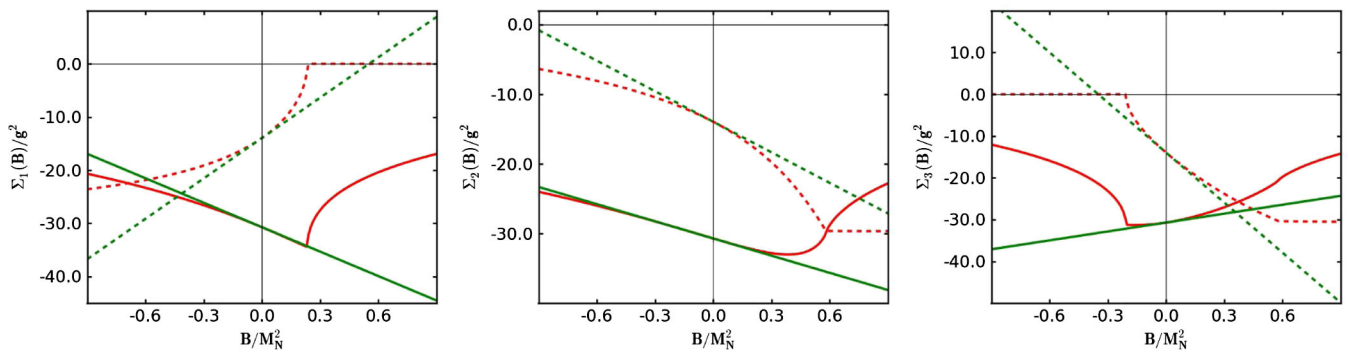


FIG. 3 (color online). Self-energies of a resonance in an external magnetic field B . The linear green lines correspond to the linear approximation Eq. (11) while the curved red lines to Eqs. (35). The solid lines show the real parts and the dotted lines the imaginary parts.

IV. NUCLEON SELF-ENERGY

We apply now the BFT to a more involved situation, namely, the nucleon self-energy in the $SU(2)$ chiral perturbation theory of [23]:

$$\mathcal{L}_{N\pi} = \bar{N}(i\not{D} - M_N)N - \frac{g_A}{2f_\pi} \bar{N}\tau^a(\not{D}^{\mu\nu}\pi^b)\gamma_5 N + \frac{1}{2}(D_\mu^{\mu\nu}\pi^b)(D_{\mu\nu}^{\mu\nu}\pi^c) - \frac{1}{2}m_\pi^2\pi_a\pi^a. \quad (44)$$

The covariant derivatives are given in the Appendix and the nucleon axial-vector and the pion decay constants are $g_A = 1.27$ and $f_\pi = 92.4$ MeV. We consider the two graphs Σ_1 and Σ_2 in Fig. 1 and obtain for the nucleon the following unrenormalized self-energies in $d = 4 - 2\epsilon$ dimensions:

$$\Sigma_1^N(B) = i\left(\frac{g_A}{2f_\pi}\right)^2 M_N \int_0^1 dz [-M_N^2(1-z)^3 J_2 + (-6 + 3z)J_1 + (3-z)\epsilon J_1 + Bz^2(3-z)J_2], \quad (45)$$

$$\Sigma_2^N(B) = i\left(\frac{g_A}{2f_\pi}\right)^2 M_N \int_0^1 dz [-M_N^2(1-z)^3 J_2 + (-6 + 3z)J_1 + (3-z)\epsilon J_1 + B(2(1-z)^4 M_N^2 J_3 + (3-8z+6z^2-z^3)J_2 - (3-4z+z^2)\epsilon J_2)]. \quad (46)$$

The loop integrals $J_i = J_i(\mathcal{M}_N)$ with $\mathcal{M}_N = zm_\pi^2 + (1-z)^2 M_N^2 + z(1-z)B$ are listed in the Appendix. The expressions Σ_1 and Σ_2 only differ by B dependent terms and we write for the nucleon self-energies:

$$\Sigma_p(B) = 2\Sigma_1(B) + \Sigma_2(B), \quad (47)$$

$$\Sigma_n(B) = 3\Sigma_1(0) - 2\Sigma_1(B) + 2\Sigma_2(B). \quad (48)$$

By integrating the Feynman parameter we get the \widetilde{MS} renormalized proton self-energy

$$\Sigma_p(B) = \frac{M_N C_N}{24(1-B)^4} \left[n_1 + n_2 \ln \mu + \frac{n_3}{\sqrt{4\mu^2 - (B + \mu^2)^2}} \arccos \frac{B + \mu^2}{2\mu} \right], \quad (49)$$

$$n_1(B, \mu) = 36 - 156B + 236B^2 - 135B^3 + 12B^4 + 7B^5 + (72 - 252B)\mu^2 + \mathcal{O}(B^2), \quad (50)$$

$$n_2(B, \mu) = -24B^3 + 42B^4 - 12B^5 + 96B\mu^2 + (-144 + 348B)\mu^4 + (36 - 72B)\mu^6 + \mathcal{O}(B^2), \quad (51)$$

$$n_3(B, \mu) = -24B^2 + 42B^3 - 12B^4 + 120B\mu^2 + (-36 + 72B)\mu^4 + \mathcal{O}(B^2), \quad (52)$$

with $C_N = (\frac{g_A M_N}{4\pi f_\pi})^2$. We give here only terms up to $\mathcal{O}(B^2)$ or constant in μ and list in the Appendix the full coefficients $n_i(B, \mu)$. By setting $B = 0$ we recover the normal nucleon \widetilde{MS} renormalized B χ PT self-energy [24,25]:

$$\Sigma_p(0) = \frac{3}{2} M_N C_N \left[1 + 2\mu^2 - 2\mu^3 \sqrt{1 - \frac{\mu^2}{4}} \arccos \frac{\mu}{2} - \mu^4 \ln \mu \right]. \quad (53)$$

The chiral expansion of the nucleon mass is

$$M_N(B) = \dot{M}_N - 4\dot{c}_1 m_\pi^2 + \Sigma_N^{(3)}(B) - \frac{\dot{\kappa}_N}{2M_N} B, \quad (54)$$

where \dot{M}_N , \dot{c}_1 and $\dot{\kappa}_N$ are the low-energy constants for the nucleon mass and its AMM. The μ^0 and μ^2 terms in Eq. (53) break the usual power counting scheme [23] where e.g. the EOMS renormalization scheme [26] is one way to deal with this problem. The general behavior of the self-energy in this section is similar to the nucleon self-energy of the last section for pseudoscalar $N - \pi$ couplings.

In Fig. 4 we show the proton self-energy as a function of the magnetic field B for the phenomenological values. In the case of the linear approximation we use the AMM obtained from the three-point method, i.e. defined by $\kappa = F_2(0)$ via the matrix element

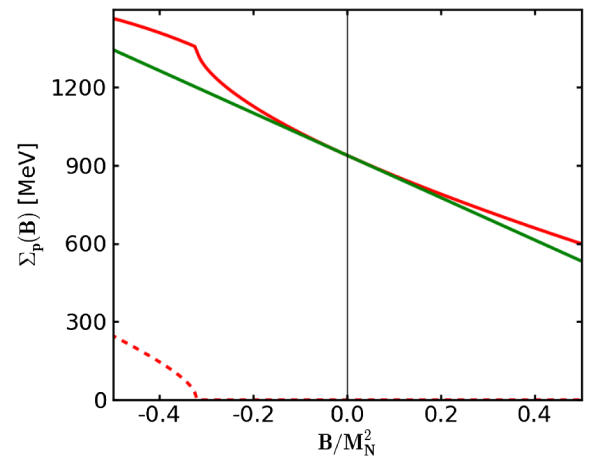


FIG. 4 (color online). Proton self-energy as function of a magnetic field B for $m_\pi = 139$ MeV and $M_N = 939$ MeV. The solid red line is the result of Eq. (49) and the solid linear green line the linear approximation $\Sigma_p(B) = M_N - \frac{\kappa}{2M_N} B$ with $\kappa = 1.73$. The dashed line is the imaginary part of Eq. (49).

$$\begin{aligned} & \langle N(p') | \bar{\Psi}(0) \gamma^\mu \Psi(0) | N(p) \rangle \\ &= \bar{u}(p') \left[\gamma^\mu F_1(q^2) + \frac{i \sigma^{\mu\nu} q_\nu}{2M_N} F_2(q^2) \right] u(p), \end{aligned} \quad (55)$$

with $q = p' - p$ as the momentum transfer. The explicit results for the nucleon graphs in the second row of Fig. 1 are

$$\begin{aligned} \kappa_1^N &= \frac{1}{i} \left(\frac{g_A M_N}{2f_\pi} \right)^2 \int_0^1 dz 2z [(-6 + 12z - 4z^2)J_2 \\ &+ (3 - 4z + z^2)\varepsilon J_2 - 2M_N^2(1 - z)^4 J_3] \end{aligned} \quad (56)$$

$$\begin{aligned} \kappa_2^N &= \frac{1}{i} \left(\frac{g_A M_N}{2f_\pi} \right)^2 \int_0^1 dz 2[(3 - 14z + 15z^2 - 4z^3)J_2 \\ &- (3 - 7z + 5z^2 - z^3)\varepsilon J_2 + 2M_N^2(1 - z)^5 J_3] \end{aligned} \quad (57)$$

with $J_i = J_i(\mathcal{M})$ and $\mathcal{M} = zm_\pi^2 + (1 - z)^2 M_N^2$ [11]. Extracting the AMM from the above self-energy yields identical results. For example this can be seen for κ_1^N literally even before the Feynman parameter integration:

$$\begin{aligned} \kappa_1^{N(\text{BFT})} &= \frac{1}{i} \left(\frac{g_A M_N}{2f_\pi} \right)^2 \int_0^1 dz 2z [(-6 + 9z - 3z^2)J_2 \\ &+ z(3 - z)J_2 + (3 - 4z + z^2)\varepsilon J_2 \\ &- 2M_N^2(1 - z)^4 J_3]. \end{aligned} \quad (58)$$

The two J_2 integrals add up to the same expression in Eq. (56). However, in the case of the three-point function method, e.g., the J_2 contributions come purely from tensor integrals whereas in the case of the BFT method it is a combination of tensor and scalar-loop-integrals. As we see for the infinite volume case this difference is not important. Tensor-integrals do not appear in [15] where the loop-integrals of the AMM obtained from the BFT or the three-point function method are the same. The above observed different loop-integral combinations might yield different finite volume corrections and would imply that these corrections calculated from the self-energy or the vector-current matrix element may differ. However, a quantitative study of finite volume effects is beyond the scope of this work.

V. DELTA(1232) SELF-ENERGY

We consider now the $\Delta^+(1232)$ -isobar and concentrate on the graphs that give its decay width. We take the following Lagrangian [24]:

$$\begin{aligned} \mathcal{L}_{\Delta\pi} &= \bar{\Delta}_\mu (i\gamma^{\mu\nu\alpha} D_\alpha - M_\Delta \gamma^{\mu\nu}) \Delta_\nu \\ &+ i \frac{h_A}{2f_\pi M_\Delta} \bar{N} T^a \gamma^{\mu\nu\lambda} (D_\mu \Delta_\nu) (D_\lambda^{ab} \pi^b) + \text{H.c.}, \end{aligned} \quad (59)$$

and obtain the relevant self-energies as:

$$\Sigma_1^\Delta(B) = \frac{1}{i} M_\Delta \left(\frac{h_A}{2f_\pi} \right)^2 \frac{1}{2} \int_0^1 dz [(z + r)J_1 - B(z + r)z^2 J_2], \quad (60)$$

$$\begin{aligned} \Sigma_2^\Delta(B) &= \frac{1}{i} M_\Delta \left(\frac{h_A}{2f_\pi} \right)^2 \frac{1}{2} \int_0^1 dz [(z + r)J_1 \\ &- B(z + r)(1 - z)^2 J_2], \end{aligned} \quad (61)$$

$$\mathcal{M}_\Delta = z\mu^2 + (1 - z)r^2 - z(1 - z) + \mathcal{B}_i, \quad (62)$$

with $\mathcal{B}_1 = +z(1 - z)\mathcal{B}$ and $\mathcal{B}_2 = -(1 - z)^2\mathcal{B}$ and all other definitions given in the Appendix. Integrating these expressions yield

$$\begin{aligned} \Sigma_1^\Delta(B) \cdot \frac{144}{M_\Delta C_\Delta} &= \mathcal{A}_1(B) + 48[2(r + \alpha_1)\lambda_1^2 \\ &+ \mathcal{B}(3(r + \alpha_1)\alpha_1^2 + (\alpha_1 - r)\lambda_1^2)]\Omega_1(B), \end{aligned} \quad (63)$$

$$\begin{aligned} \Sigma_2^\Delta(B) \cdot \frac{144}{M_\Delta C_\Delta} &= \mathcal{A}_2(B) + 48[2(r + \alpha_2)\lambda_2^2 \\ &+ \mathcal{B}(3r + 3\alpha_2 - 6r\alpha_2 \\ &- (3\alpha_2^2 + 1)(2 + r - \alpha_2)\lambda_2^2)]\Omega_2(B), \end{aligned} \quad (64)$$

$$\Omega_i(B) = \sqrt{\lambda_i^2} \left(\text{arctanh} \frac{\beta_i}{\sqrt{\lambda_i^2}} + \text{arctanh} \frac{\alpha_i}{\sqrt{\lambda_i^2}} \right), \quad (65)$$

with $C_\Delta = (\frac{h_A M_\Delta}{8f_\pi \pi})^2$ and the analytic parts \mathcal{A}_i also listed in the Appendix. With these two expressions we can also write the self-energy of the different isospin states as

$$\Sigma_{\Delta^{++}}(B) = -\Sigma_1^\Delta(0) + \Sigma_1^\Delta(B) + \Sigma_2^\Delta(B), \quad (66)$$

$$\Sigma_{\Delta^+}(B) = \frac{1}{3} \Sigma_1^\Delta(B) + \frac{2}{3} \Sigma_2^\Delta(B), \quad (67)$$

$$\Sigma_{\Delta^0}(B) = \Sigma_1^\Delta(0) - \frac{1}{3} \Sigma_1^\Delta(B) + \frac{1}{3} \Sigma_2^\Delta(B), \quad (68)$$

$$\Sigma_{\Delta^-}(B) = 2\Sigma_1^\Delta(0) - \Sigma_1^\Delta(B). \quad (69)$$

In Fig. 5 we show the $\Delta^+(1232)$ self-energy as function of the magnetic field B for the phenomenological parameters together with the linear approximation as obtained from the three-point function method. The cusp is from Σ_1 while the second cusp of Σ_2 is not present for $m_\pi = 139$ MeV. However it emerges on the $B < 0$ side for larger pion masses and both cusps fall on $B = 0$ for $m_\pi = M_\Delta - M_N$. The imaginary parts read

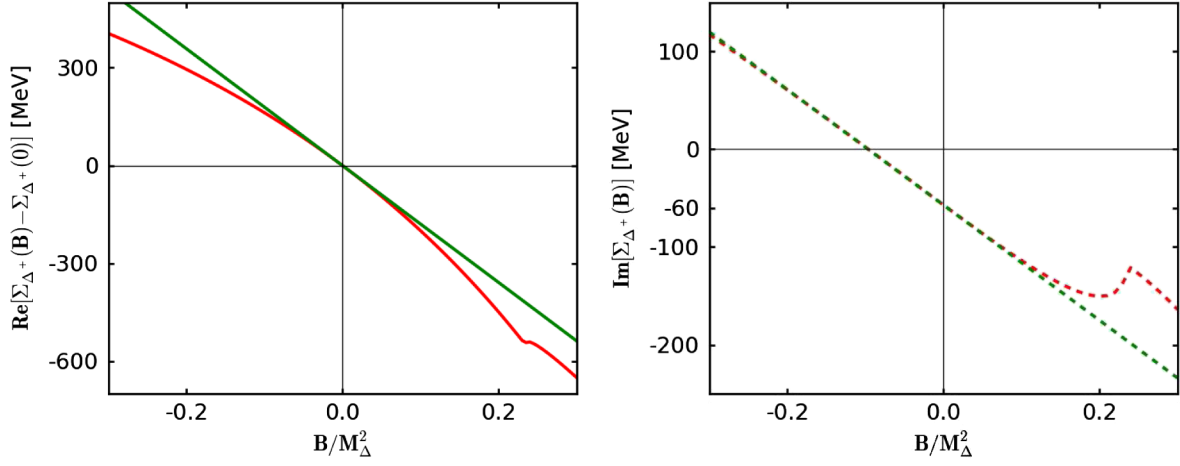


FIG. 5 (color online). The $\Delta^+(1232)$ -isobar self-energy loop results as function of a magnetic field B for $m_\pi = 139$ MeV, $M_N = 939$ MeV and $M_\Delta = 1232$ MeV. The left pictures shows the real part and the right one the imaginary part. The curved red solid lines are from Eq. (62) while the linear green lines correspond to the linear approximation $\Sigma_\Delta(B) = M_\Delta - \frac{\kappa_\Delta}{2M_\Delta} B$.

$$\begin{aligned} \text{Im}\Sigma_1(B) \cdot \frac{3}{\pi M_\Delta C_\Delta} \\ = -2(1 - \mathcal{B})(r + \alpha_1)\lambda_1^3 \\ - \mathcal{B}\lambda_1[3\alpha_1(\alpha_1^2 + \lambda_1^2) + r(3\alpha_1^2 + \lambda_1^2)], \end{aligned} \quad (70)$$

$$\begin{aligned} \text{Im}\Sigma_2(B) \cdot \frac{3}{\pi M_\Delta C_\Delta} \\ = -2(1 - \mathcal{B})(r + \alpha_2)\lambda_2^3 - \mathcal{B}\lambda_2[-6\alpha_2^2 + 3\alpha_2^3 - 2\lambda_2^2 \\ + 3\alpha_2(1 + \lambda_2^2) + r(3 - 6\alpha_2 + 3\alpha_2^2 + \lambda_2^2)], \end{aligned} \quad (71)$$

where the $\Delta^+(1232)$ decay width, experimentally given by $\Gamma_\Delta \approx 120$ MeV, is obtained from $\Gamma = -2 \text{Im}\Sigma(B=0)$. The slope of the imaginary part at $B=0$ in Fig. 5 is consistent with [27] and we obtain a vanishing decay width at

$$\begin{aligned} \mathcal{B} = -\frac{(1 - 2r + r^2 - \mu^2)(1 + 2r + r^2 - \mu^2)}{2(1 + r - 2r^3 + 3r^4 + 2r\mu^2 + 3\mu^4 - 2r^2(1 + 3\mu^2))} \\ + \mathcal{O}(\mathcal{B}^2). \end{aligned} \quad (72)$$

The magnetic moment from the three-point function method is again defined through the vector matrix element by $\kappa = F_2(0)$ and

$$\begin{aligned} \langle \Delta(p') | \bar{\Psi}(0) \gamma^\mu \Psi(0) | \Delta(p) \rangle \\ = -\bar{u}_\alpha(p') \left\{ \left[F_1^\Delta \gamma^\mu + \frac{i\sigma^{\mu\nu} q_\nu}{2M_\Delta} F_2^\Delta \right] g^{\alpha\beta} \right. \\ \left. + \left[F_3^\Delta \gamma^\mu + \frac{i\sigma^{\mu\nu} q_\nu}{2M_\Delta} F_4^\Delta \right] \frac{q^\alpha q^\beta}{4M_\Delta^2} \right\} u_\beta(p), \end{aligned} \quad (73)$$

with the results [11]:

$$\kappa_1^\Delta = \frac{1}{i} \left(\frac{h_A M_\Delta}{2f_\pi} \right)^2 \int_0^1 dz 2z \left[-\frac{1}{2}z + z^2 - \frac{1}{2}r + zr \right] J_2, \quad (74)$$

$$\begin{aligned} \kappa_2^\Delta = \frac{1}{i} \left(\frac{h_A M_\Delta}{2f_\pi} \right)^2 \int_0^1 dz 2(1 - z) \\ \times [(1 + r)(1 - z) - (1 - z)^2] J_2, \end{aligned} \quad (75)$$

with $J_i = J_i(\mathcal{M}_\Delta)$ and $\mathcal{M}_\Delta = z\mu^2 + (1 - z)r^2 - z(1 - z)$. The results of the BFT method agree in this form literally.

From $\sqrt{\lambda_1^2}$ in Eq. (65) we obtain the condition

$$\left| \frac{eB}{2M_\Delta} \right| \ll |M_\Delta - (M_N + m_\pi)| \quad (76)$$

for expanding the $\Delta(1232)$ -isobar self-energies in small magnetic fields [15].

VI. SUMMARY

We investigated the self-energies of particles placed in a constant electromagnetic (EM) field. Explicitly, we applied the EM background field technique (BFT) once to the situation of stable and unstable spin-1/2 particles coupling to (pseudo-) scalar fields and once to the nucleon and $\Delta(1232)$ -isobar baryons in the $SU(2)$ chiral perturbation theory (B χ PT). We obtained the self-energies of these particles as function of the external constant magnetic field B and calculated from these the anomalous magnetic moments (AMM) by the linear energy shift. We summarize our findings as:

- (i) Self-energies of Dirac particles coupling to (pseudo-) scalar fields: We investigated all three types of Feynman graphs that can appear in the one-loop BFT. The self-energies generally depend nonanalytically on B where for stable particles the actual

nonanalytic points are unproblematic for defining the AMM by the linear energy shift. These points depend on the masses and charges of the involved particles and give three different conditions for resonances on when their self-energies can be expanded for weak B . One of these conditions was reported earlier. The self-energy formulas contain those $\mathcal{O}(B^2)$ terms that keep the nonanalytical dependence intact, in contrast to the one-photon approximation. However, they omit some $\mathcal{O}(B^2)$ contributions where we estimated for the nucleon-pion system with pseudoscalar couplings that these contributions are small for magnetic fields of $|B| < \frac{1}{5}M_N^2$ with M_N as the nucleon mass.

- (ii) Self-energies of the nucleon and $\Delta(1232)$ -isobar in $B\chi$ PT: We derived the formulas for the nucleon and $\Delta(1232)$ -isobar self-energies depending on the pion mass and the magnetic field. We recover the expressions as obtained from the three-point function method as well as the condition on when the $\Delta(1232)$ -isobar magnetic moment is well defined by the linear energy shift. Furthermore, we saw that the AMM expressions have different tensor- and scalar-loop integral combinations depending on whether the AMM is derived by the three-point function method or from the self-energy. In the infinite volume these combinations add up to the same AMM expressions.

ACKNOWLEDGMENTS

The author is thankful to B. Tiburzi, V. Pascalutsa, and M. Vanderhaeghen for valuable discussions and critical comments.

APPENDIX: NOTATION

We use the following notations: $\tilde{d}l = d^n l / (4\pi)^n$ with $n = 4 - 2\epsilon$ dimensions,

$$\mu = m/M_{\text{ex}} \quad r = M_{\text{in}}/M_{\text{ex}} \quad \mathcal{B} = B/M_{\text{ex}}^2. \quad (\text{A1})$$

The covariant derivatives are

$$D_\mu^{ab} \pi^b = \delta^{ab} \partial_\mu \pi^b + ie Q_\pi^{ab} A_\mu \pi^b, \quad (\text{A2})$$

$$D_\mu N = \partial_\mu N + ie Q_N A_\mu N + \frac{i}{4f_\pi^2} \epsilon^{abc} \tau^a \pi^b (\partial_\mu \pi^c), \quad (\text{A3})$$

$$D_\mu \Delta_\nu = \partial_\mu \Delta_\nu + ie Q_\Delta A_\mu \Delta_\nu + \frac{i}{2f_\pi^2} \epsilon^{abc} \mathcal{T}^a \pi^b (\partial_\mu \pi^c), \quad (\text{A4})$$

with the operators $Q_N = (1 + \tau^3)/2$ and $Q_\pi^{ab} = -i\epsilon^{ab3}$. The results for the loop integration in infinite volume and dimensional regularization with $L = -\frac{1}{\epsilon} + \gamma_E + \ln \frac{M_{\text{sc}}^2}{4\pi\Lambda^2}$ are

$$\begin{aligned} J_1(\mathcal{M}) &= \frac{-i}{(4\pi)^2} m_{\text{sc}}^2 \tilde{\mathcal{M}} [L - 1 + \ln \tilde{\mathcal{M}}], \\ J_2(\mathcal{M}) &= \frac{-i}{(4\pi)^2} [L + \ln \tilde{\mathcal{M}}], \\ J_3(\mathcal{M}) &= \frac{-i}{(4\pi)^2} \frac{1}{2m_{\text{sc}}^2} \frac{1}{\tilde{\mathcal{M}}}. \end{aligned} \quad (\text{A5})$$

The corresponding parts of the nucleon and $\Delta(1232)$ self-energies are

$$\begin{aligned} n_1(\mathcal{B}, \mu) &= 36 - 156\mathcal{B} + 236\mathcal{B}^2 - 135\mathcal{B}^3 + 12\mathcal{B}^4 + 7\mathcal{B}^5 \\ &\quad + (72 - 252\mathcal{B} + 321\mathcal{B}^2 - 186\mathcal{B}^3 + 45\mathcal{B}^4)\mu^2 \\ &\quad + (6\mathcal{B}^2 - 6\mathcal{B}^3)\mu^4 \end{aligned} \quad (\text{A6})$$

$$\begin{aligned} n_2(\mathcal{B}, \mu) &= -24\mathcal{B}^3 + 42\mathcal{B}^4 - 12\mathcal{B}^5 \\ &\quad + (96\beta - 180\beta^2 + 60\beta^3 + 12\beta^4 - 12\beta^5)\mu^2 \\ &\quad + (-144 + 348\mathcal{B} - 270\mathcal{B}^2 + 120\mathcal{B}^3 - 18\mathcal{B}^4)\mu^4 \\ &\quad + (36 - 72\mathcal{B} + 12\mathcal{B}^2)\mu^6 + 6\mathcal{B}^2\mu^8 \end{aligned} \quad (\text{A7})$$

$$\begin{aligned} n_3(\mathcal{B}, \mu) &= -24\mathcal{B}^2 + 42\mathcal{B}^3 - 12\mathcal{B}^4 \\ &\quad + (120\mathcal{B} - 294\mathcal{B}^2 + 216\mathcal{B}^3 - 60\mathcal{B}^4)\mu^2 \\ &\quad + (-36 + 72\mathcal{B} - 24\mathcal{B}^2 + 6\mathcal{B}^3)\mu^4 - 6\mathcal{B}^2\mu^6 \end{aligned} \quad (\text{A8})$$

$$\begin{aligned} \mathcal{A}(B) &= 27 + 40r - 68\alpha - 120r\alpha + 42\alpha^2 + 120r\alpha^2 + 12\alpha^3 - 54\lambda^2 - 168r\lambda^2 - 60\alpha\lambda^2 + (-18 + 48\alpha - 36\alpha^2 + 36\lambda^2 \\ &\quad - 24r(1 - 3\alpha + 3\alpha^2 - 3\lambda^2))\ln(1 - \mathcal{B}) + (-24r\alpha^3 - 6\alpha^4 + 72r\alpha\lambda^2 + 36\alpha^2\lambda^2 + 18\lambda^4)\ln(\alpha^2 - \lambda^2) \\ &\quad + (-18 + 48\alpha - 36\alpha^2 + 6\alpha^4 + 36\lambda^2 - 36\alpha^2\lambda^2 - 18\lambda^4 + 24r(\alpha - 1)((\alpha - 1)^2 - 3\lambda^2))\ln(\beta^2 - \lambda^2) \end{aligned} \quad (\text{A9})$$

$$\begin{aligned} \mathcal{A}_1(B) &= [\mathcal{A}(B) + \mathcal{B}(-36 - 56r + 56\alpha + 96r\alpha - 60\alpha^2 - 168r\alpha^2 - 48\alpha^3 + 36\lambda^2 + 120r\lambda^2 - 48\alpha\lambda^2 \\ &\quad + \sqrt{\lambda^2}\Omega(144r\alpha^2 + 144\alpha^3 - 48r\lambda^2 + 48\alpha\lambda^2) + 12(3 - 4\alpha + 3\alpha^2 - 3\lambda^2 + r(4 - 6\alpha + 6\alpha^2 - 6\lambda^2))\ln(1 - \mathcal{B}) \\ &\quad + (48r\alpha^3 + 24\alpha^4 + 72\alpha^2\lambda^2)\ln(\alpha^2 - \lambda^2) - 12(4\alpha + 2\alpha^4 + 3(\lambda^2 - 1) + \alpha^2(6\lambda^2 - 3) \\ &\quad + r(6(\alpha - \alpha^2 + \lambda^2) - 4 + 4\alpha^3))\ln(\beta^2 - \lambda^2)]_{\alpha, \beta, \lambda \rightarrow \alpha_1, \beta_1, \lambda_1} \end{aligned} \quad (\text{A10})$$

$$\begin{aligned}
\mathcal{A}_2(B) = & [\mathcal{A}(B) + \mathcal{B}(-40 - 128r + 32\alpha + 240r\alpha + 36\alpha^2 - 168r\alpha^2 - 48\alpha^3 + 132\lambda^2 + 120r\lambda^2 - 48\alpha\lambda^2 \\
& + 12(2 - 4\alpha + 3\alpha^2 - 3\lambda^2 + r(4 - 6\alpha + 6\alpha^2 - 6\lambda^2))\ln(1 - \mathcal{B}) + (72r\alpha + 36\alpha^2 - 72r\alpha^2 - 48\alpha^3 + 48r\alpha^3 \\
& + 24\alpha^4 + 36\lambda^2 - 72r\lambda^2 - 144\alpha\lambda^2 + 72\alpha^2\lambda^2)\ln(\alpha^2 - \lambda^2) - 24(-1 + \alpha)^2(-1 + 2r(-1 + \alpha) + \alpha^2 + 3\lambda^2) \\
& \times \ln(\beta^2 - \lambda^2)]_{\alpha, \beta, \lambda \rightarrow \alpha_2, \beta_2, \lambda_2}
\end{aligned} \tag{A11}$$

-
- [1] J. D. Bratt *et al.* (LHPC Collab.), *Phys. Rev. D* **82**, 094502 (2010).
- [2] C. Alexandrou, M. Brinet, J. Carbonell, M. Constantinou, P. A. Harraud *et al.*, *Phys. Rev. D* **83**, 094502 (2011).
- [3] S. N. Syritsyn, J. D. Bratt, M. F. Lin, H. B. Meyer, J. W. Negele *et al.* (LHPC Collaboration), *Phys. Rev. D* **81**, 034507 (2010).
- [4] S. Collins *et al.*, *Phys. Rev. D* **84**, 074507 (2011).
- [5] C. W. Bernard, T. Draper, K. Olynyk, and M. Rushton, *Phys. Rev. Lett.* **49**, 1076 (1982).
- [6] G. Martinelli, G. Parisi, R. Petronzio, and F. Rapuano, *Phys. Lett. B* **116**, 434 (1982).
- [7] F. X. Lee, R. Kelly, L. Zhou, and W. Wilcox, *Phys. Lett. B* **627**, 71 (2005).
- [8] C. Aubin, K. Orginos, V. Pascalutsa, and M. Vanderhaeghen, *Phys. Rev. D* **79**, 051502 (2009).
- [9] W. Detmold, B. C. Tiburzi, and A. Walker-Loud, *Phys. Rev. D* **81**, 054502 (2010); arXiv:1108.1698.
- [10] F. J. Jiang and B. C. Tiburzi, *Phys. Rev. D* **81**, 034017 (2010).
- [11] T. Ledwig, J. Martin-Camalich, V. Pascalutsa, and M. Vanderhaeghen, *Phys. Rev. D* **85**, 034013 (2012).
- [12] J. Hu, F.-J. Jiang, and B. Tiburzi, *Phys. Lett. B* **653**, 350 (2007); B. Tiburzi, *Phys. Rev. D* **77**, 014510 (2008).
- [13] B. Tiburzi, *Phys. Lett. B* **674**, 336 (2009).
- [14] B. Tiburzi, *Nucl. Phys. A* **814**, 74 (2008).
- [15] T. Ledwig, V. Pascalutsa, and M. Vanderhaeghen, *Phys. Rev. D* **82**, 091301 (2010).
- [16] G. Couture and J. N. Ng, *Z. Phys. C* **35**, 65 (1987).
- [17] E. N. Argyres, G. Katsilieris, A. B. Lahanas, C. G. Papadopoulos, and V. C. Spanos, *Nucl. Phys. B* **391**, 23 (1993).
- [18] V. Pascalutsa and M. Vanderhaeghen, *Phys. Rev. Lett.* **94**, 102003 (2005).
- [19] S. P. Martin, arXiv:hep-ph/9709356.
- [20] H. K. Dreiner, H. E. Haber, and S. P. Martin, *Phys. Rep.* **494**, 1 (2010).
- [21] J. S. Schwinger, *Phys. Rev.* **82**, 664 (1951); C. M. Sommerfield, *Ann. Phys. (N.Y.)* **5**, 26 (1958).
- [22] T. Ledwig, V. Pascalutsa, and M. Vanderhaeghen, *Phys. Lett. B* **690**, 129 (2010).
- [23] J. Gasser, M. E. Sainio, and A. Svarc, *Nucl. Phys. B* **307**, 779 (1988).
- [24] V. Pascalutsa and M. Vanderhaeghen, *Phys. Lett. B* **636**, 31 (2006).
- [25] V. Pascalutsa and M. Vanderhaeghen, *Phys. Rev. D* **73**, 034003 (2006).
- [26] J. Gegelia and G. Japaridze, *Phys. Rev. D* **60**, 114038 (1999); J. Gegelia, G. Japaridze, and X. Q. Wang, *J. Phys. G* **29**, 2303 (2003); T. Fuchs, J. Gegelia, G. Japaridze, and S. Scherer, *Phys. Rev. D* **68**, 056005 (2003).
- [27] V. Pascalutsa and M. Vanderhaeghen, *Phys. Rev. Lett.* **94**, 102003 (2005).